Published in final edited form as:
Blood. 2011 July 28; 118(4): 1041–1051. doi:10.1182/blood-2011-02-338848.

Modeling the evolution of *ETV6-RUNX1*-induced B-cell precursor acute lymphoblastic leukemia in mice

Louise van der Weyden[1,*], **George Giotopoulos**[2], **Alistair G. Rust**[1], **Louise S. Matheson**[3], **Frederik W. van Delft**[4], **Jun Kong**[1], **Anne E. Corcoran**[3], **Mel F. Greaves**[4], **Charles G. Mullighan**[5], **Brian J. Huntly**[2,α], and **David J. Adams**[1,α]

[1]Wellcome Trust Sanger Institute, Wellcome Trust Genome Campus, Hinxton, Cambridge, CB10 1HH, U.K.

[2]Cambridge Institute for Medical Research, Wellcome Trust/MRC Building, Addenbrooke's Hospital, Hills Road, Cambridge, CB2 0XY, U.K.

[3]The Babraham Institute, Babraham Research Campus, Cambridge CB22 3AT, U.K.

[4]The Institute of Cancer Research, Section of Haemato-Oncology, Cotswold Road, Belmont, Sutton, Surrey, SM2 5NG, U.K.

[5]St. Jude Children's Research Hospital, 262 Danny Thomas Place, Memphis, TN 38105-3678, U.S.A.

Abstract

The t(12;21) translocation which generates the *ETV6-RUNX1* (*TEL-AML1*) fusion gene, is the most common chromosomal rearrangement in childhood cancer and is exclusively associated with B-cell precursor acute lymphoblastic leukemia (BCP-ALL). The translocation arises *in utero* and is necessary but insufficient for the development of leukemia. SNP array analysis of *ETV6-RUNX1* patient samples have identified multiple additional genetic alterations, however the role of these lesions in leukemogenesis remains undetermined. Moreover, murine models of *ETV6-RUNX1* ALL that faithfully recapitulate the human disease are lacking. To identify novel genes that co-operate with *ETV6-RUNX1* in leukemogenesis, we generated a mouse model that uses the endogenous *Etv6* locus to co-express the *ETV6-RUNX1* fusion and *Sleeping Beauty* (SB) transposase. An insertional mutagenesis screen was performed by intercrossing these mice with those carrying a SB transposon array. In contrast to previous models, a substantial proportion (20%) of the offspring developed BCP-ALL. Isolation of the transposon insertion sites identified genes known to be associated with BCP-ALL, including *Ebf1* and *Epor*, in addition to other novel candidates. This is the first mouse model of *ETV6-RUNX1* to develop BCP-ALL and provides important insights into the cooperating genetic alterations in *ETV6-RUNX1* leukemia.

[*]Correspondence: Louise van der Weyden, Experimental Cancer Genetics, Wellcome Trust Sanger Institute, Wellcome Trust Genome Campus, Hinxton, Cambridge, CB10 1HH, United Kingdom, Tel: +44-1223-834-244, Fax: +44-1223-496-802, lvdw@sanger.ac.uk.
[α]These authors contributed equally.

Authorship:

Contribution: LvdW conceived and performed research, collected, analyzed and interpreted data and wrote the manuscript; GG performed research, collected, analyzed and interpreted data and assisted in writing the manuscript, AGR performed statistical analysis and assisted in writing the manuscript, LSM performed research, analyzed data and edited the manuscript, FWvD analyzed data and edited the manuscript, JK performed research, AEC analyzed data and edited the manuscript, MG analyzed data and edited the manuscript, CGM performed research, analyzed data and edited the manuscript, BJH conceived and performed research, collected, analyzed and interpreted data and assisted in writing the manuscript, DJA conceived and performed research, interpreted data and assisted in writing the manuscript.

Conflict-of-interest disclosure: The authors declare no competing financial interests.

Europe PMC Funders Author Manuscripts

Keywords

ETV6-RUNX1; leukemia; precursor-B cell; insertional mutagenesis

Introduction

The *ETV6-RUNX1* fusion gene generated by the t(12;21)(p13;q22) chromosomal translocation,[1] is the most prevalent fusion gene in childhood acute lymphoblastic leukemias (ALL), the most common malignancy of childhood. It occurs in around 20% of cases, and is almost exclusively associated with the common B-cell precursor subset of ALL (also known as common ALL, cALL).[2] The fusion gene arises during fetal hematopoiesis in a B-cell precursor,[3] giving rise to a preleukemic cALL-propagating cell that was recently identified by the surface phenotype $CD34^{+}CD38^{-/low}CD19^{+}$.[4-5] However, the frequency of individuals carrying the *ETV6-RUNX1* fusion gene at birth considerably exceeds the number of patients presenting with clinically overt ALL,[6] and twin studies and retrospective analysis of neonatal blood spots from ALL patients indicate that *ETV6-RUNX1*-expressing fetal clones expand and can persist in a clinically covert state for more than a decade.[5] Taken together, this indicates the requirement for additional secondary (postnatal) genetic events ('hits') for the development of ALL.

ETV6-RUNX1+ ALL at diagnosis is characterized by multiple copy number alterations (4-7 per case). These commonly include deletions in genes regulating B cell differentiation or cell cycling[7] and studies on identical twins with concordant ALL indicate that these genetic events are secondary to *ETV6-RUNX1* fusion, and probably occur post-natally.[8] In agreement with these clinical observations, animal models of *ETV6-RUNX1* in both mice and zebrafish have shown that expression of the *ETV6-RUNX1* fusion alone is insufficient for leukemogenesis, yet similar to the *RUNX1-RUNX1T1* fusion,[9] leukemia may occur following the acquisition of co-operating mutations.[10-14] However, these models of *ETV6-RUNX1* leukemia have not been suitable for the identification of co-operating mutations for two reasons. First, they do not accurately recapitulate the precursor B-cell phenotype associated with expression of the *ETV6-RUNX1* fusion. Secondly, the models either utilize mutations already known to co-occur in *ETV6-RUNX1* expressing ALL (such as deletion of the *CDKN2A [p16]* and *p19* genes[10]) which provide no further pathogenetic information, or use agents such as N-ethyl-N-nitrosourea to induce secondary mutations, that are difficult to identify. To overcome these limitations, we have developed a new mouse model of *ETV6-RUNX1* ALL, in which expression of the fusion gene is driven from the endogenous *Etv6* promoter, and is linked to expression of the *Sleeping Beauty* (SB) transposase. This not only allows for expression of the fusion gene at endogenous levels, but also recapitulates expression of the fusion gene in the pattern of endogenous *Etv6*, and allows forward mutagenesis to occur in the same cellular compartment.

Our model demonstrates that in the presence of mutations induced by the SB transposon, mice carrying the *ETV6-RUNX1* allele can develop B-cell precursor ALL (BCP-ALL). Furthermore, transposon insertions can be used to identify gene mutations that co-operate with *ETV6-RUNX1* in leukemogenesis. This model therefore represents a unique tool for both studying the biology of this common disease and for identifying mutations that mediate development of ALL in cooperation with *ETV6-RUNX1*.

Europe PMC Funders Author Manuscripts

Europe PMC Funders Author Manuscripts

Materials and methods

Generation of ETV6-RUNX1 mice

A 10.1 kb fragment of 129S5/SvEV^{Brd} genomic DNA (NCBI m37: Chr6; 134200205-134210356) from BAC clone bMQ-66f22 was captured by recombineering into pBluescript. This fragment contained most of intron 5-6, based on the longest protein-coding transcript of *Etv6* (Ensembl ID: ENSMUST00000081028). Into the captured genomic fragment a cassette was inserted containing: a splice acceptor, exons 1-6 of human *RUNX1*, an EMCV IRES, a hyperactive variant of the *SB* transposase (*HSB5*),[15] and an FRT-flanked PGK-*PuroΔ TK* drug selection marker.[16] This entire cassette was synthesized by GENEART (GENEART AG, Regensburg, Germany) to ensure fidelity, and was flanked by *Lox*66/*Lox*71 sites (to allow Cre-mediated inactivation of the *ETV6-RUNX1* fusion gene) and *Hpa*I sites (to allow cloning into the two *Stu*I sites of the captured genomic fragment). The final targeting construct was termed *pAML-IRES-SB-puro*. Targeting was performed in E14Tg2a ES cells (129P2Ola/Hsd) and correctly targeted clones identified by southern blotting on *Stu*I digested gDNA using a 5′ Probe A (generated by PCR on gDNA using FOR: 5′-GGG CAC CTA CGA TGC ACA GAT AAA TAC ATC CGC-3′ and REV: 5′-GAG ATA GGG TCA GTC TGG AAC TGG TCG CAG GGA-3′) and 3′ Probe B (generated by PCR on gDNA using FOR 5′-TCC TCC TTG GTC CTC ATA TAA AGG TGG TA-3′ and REV: 5′-TGA GTT CTG CTG AGT TAA TGG GCC CCG GA-3′). Targeted ES cells were injected into C57BL/6J blastocysts to generate chimaeras, which were bred to 129S5/SvEv^{Brd} or C57BL/6J mice for germline transmission of the allele (*Etv6*$^{+/RUNX1}$). Mice were housed in accordance with Home Office regulations (UK). ES cell targeting of the *RUNX1-Flag* was performed in the same way (*Etv6*$^{+/RUNX1\text{-}Flag}$).

Immunoprecipitation of FLAG tagged proteins and Western blotting

Flag-tagged proteins were immunoprecipitated from whole-cell ES cell lysates using Dynabead protein G (Invitrogen, Carlsbad, CA) according to the manufacturer's instructions and Western blot analysis performed using monoclonal anti-Flag M2 antibody (Sigma-Aldrich, St. Louis, MO). Western blot was performed on whole-cell mouse bone marrow lysates using anti-SB transposase antibody (R&D Systems, Minneapolis, MN) and actin (C-11) polyclonal antibody (Santa Cruz Biotechnology, Santa Cruz, CA). The *ETV6-RUNX1-Flag* expression plasmid,[17] which was used as a positive control for immunoprecipitation and Western blotting, was kindly provided by Dr. O Williams, University College London.

Quantitative PCR

Total RNA from mouse tissue (spleen, thymus and bone marrow) was isolated using TRIzol reagent (Invitrogen) and cDNA reverse transcribed using SuperScript First-Strand RT-PCR kit (Invitrogen), according to the manufacturer's instructions. Quantitative PCR (qPCR) was performed using ABsolute™ qPCR ROX Mix kit on an ABI PRISM 7900HT sequence detection system (Applied Biosystems, Carlsbad, CA). qPCR probes with 5′ FAM and 3′ TAMRA modifications (MWG Operon, Ebersberg, Germany) were as follows: *Etv6* probe: 5′-CAC GCC ATG CCC ATT GGG AGA A-3′ (FWD primer: 5′-TCT CTA TGT CCC CAC CGG AAG-3′; REV primer: 5′-CAT AAT CCC AAA GCA GTC TAC AGT CT-3′), *Etv6-RUNX1* probe: 5′-AGC ACG CCA TGC CCA TTG GG-3′ (FWD primer: 5′-CTT GAA CCA CAT CAT GGT CTC TAT G-3′; REV primer: 5′-TCG TGC TGG CAT CTG CTAT T-3′), and *β-Actin* probe: 5′-TTT GAG ACC TTC AAC ACC CCA GCC A-3′ (FWD primer: 5′-CGT GAA AAG ATG ACC CAG ATC A-3′ and REV primer: 5′-CAC AGC CTG GAT GGC TAC GT-3′).

Embryonic lethality and leukemogenesis studies

Embryonic lethality studies were performed by timed matings of *Etv6*$^{+/RUNX1}$ mice and the embryos collected at day 10.5 of gestation. The embryos were genotyped by PCR using primers to detect the wildtype *Etv6* allele (FOR 5′-AGG CAT TGT GCA AAG AAT GAG AGA C-3′ and REV 5′-GAC CAA CCA AAC CAA ACA AAC AAA A-3′; with a 65°C annealing temperature to produce a 360 bp band) and the *Etv6*$^{+/RUNX1}$ allele (FOR 5′-AAG AAG CCA CTG CTC CAA AA-3′ and REV 5′-GCA CTT GCT CTC CCA AAG TC-3′; with a 60°C annealing temperature to produce a 376 bp band). Mice carrying the *SB* transposon array (*T2Onc*)[18] were kindly provided by Lara Collier (University of Wisconsin). Genotyping for the *T2Onc* allele and the excision PCR was performed as described previously.[16] Mice carrying the *Etv6*$^{+/RUNX1}$ and *T2Onc*$^{+/Tg}$ alleles were intercrossed and their offspring placed on tumor watch. These mice were examined twice daily for signs of disease, at which time they were sacrificed and a full necropsy performed.

Histology and immunohistochemistry

Tissues and tumors were fixed in 10% neutral-buffered formalin (NBF) at room temperature overnight. Samples were then transferred to 50% ethanol, embedded in paraffin, sectioned and stained with hematoxylin and eosin (H&E). For samples where no bone marrow was available for flow cytometric analysis of CD antigen expression, immunophenotyping was performed by immunohistochemical on formalin-fixed, paraffin-embedded tissue sections that had undergone antigen retrieval (microwaving in citrate buffer pH 6 for 20 min) using antibodies for CD3 (clone SP7; Abcam, Cambridge, UK), B220 (clone RA3-6B2, R&D systems) and MPO (DAKO, Ely, UK). Immunohistochemical signal was detected by secondary biotinylated goat anti-rabbit antibody (Vector Laboratories, Burlingame, CA), followed by Vectorstain Elite ABC kit (Vector Laboratories) according to the manufacturer's instructions.

Flow cytometric analysis

For analysis of CD antigen expression, single-cell suspensions from spleen or bone marrow were stained with combinations of Mac-1-FITC, Gr-1-PE/Cy7, Ter-119-PE, B220-AlexaFluor 647, CD4-PE/Cy7, CD19-PE, B220-PE/Cy7, CD43-PE, IgM-FITC, IgD-AlexaFluor 647, c-Kit-PE, AA4.1-PE, CD24-FITC, BP1-PE and IL7Ra-PE/Cy7 anti-mouse antibodies, obtained from BioLegend (San Diego, CA), according to the supplier's recommendations. FACS analysis was performed with a Cyan ADP Analyser (Beckman Coulter, High Wycombe UK). For the *IgH* rearrangement analysis, cells were sorted on a MoFlo Cell Sorter (Beckman Coulter).

IgH rearrangement analysis

PCR analysis was performed using Phusion High Fidelity DNA polymerase (Finnzymes, Thermo Fisher Scientific, Surrey, UK), amplifying from upstream of DQ52 (5′DQ52 FOR: TTG GGT CAC TTT CCT GCT GT) to J_H4 (J4 REV: AGA CC TGG AGA GGC CAT TCT), or from upstream of DFL/DSP genes (5′D FOR: GCA TGT CTC AAA GCA CAA TG) to J_H4 (J4 REV2: CTG AGG AGA CGG TGA CTG AG). PCR conditions used a 65°C annealing temperature and 90 sec extension time for 40 cycles. PCR products were purified (Qiagen Gel Extraction Kit, Qiagen, West Sussex, UK), cloned into pGEM-T Easy plasmid (Promega, Madison, WI), transformed into subcloning efficiency DH5α chemically competent cells (Invitrogen) and clones sequenced using either the appropriate D primer or a primer in the vector. For some samples it was necessary to perform whole genome amplification prior to *IgH* rearrangement analysis and this was performed using the GenomiPhi DNA Amplification Kit (GE Healthcare, Chalfont St Giles, UK), according to the manufacturer's instructions.

Whole genome expression profiling

Total RNA extracted from the spleens of 15 *ETV6-RUNX1* BCP-ALL cases and 3 *ETV6-RUNX1* non-diseased mice using TRIzol, according to the manufacturer's instructions. Expression profiling of the RNA was performed using a MouseWG-6 v2.0 expression beadchip kit (Illumina, Essex UK), according to the manufacturer's instructions. Data were quantile normalised[19] and analyzed using the bioconductor packages limma and lumi [http://www.bioconductor.org/]. Data were P-value adjusted to yield a sorted list of differentially expressed genes.[20] Gene annotations were further refined using ReMOAT [http://remoat.sysbiol.cam.ac.uk/]. Gene set enrichment analysis (GSEA) was performed on the differentially expressed genes using Ingenuity Pathway Analysis (IPA) software (Ingenuity Systems, Redwood City, CA).

Isolation & statistical analysis of transposon insertion sites

Isolation of the transposon insertion sites from the leukemias was performed using splinkerette PCR to produce barcoded PCR products that were pooled and sequenced as described previously.[21] The pooled PCRs were sequenced on 454 GS-FLX sequencers (Roche) platform) over four separate lanes, with one lane per restriction enzyme and a maximum of 48 leukemias per lane. Processing of 454 reads, identification of insertion sites, and Gaussian kernel convolution statistical methods used to identify common insertion sites (CIS) have been described previously.[21] The *P*-value for each CIS was adjusted by chromosome and a cut-off of $P<0.05$ was used. Any CIS on mouse chromosome 1 are not reported as this is the 'donor chromosome' where the transposon array is located. Data from this chromosome is automatically excluded from analysis due to the phenomenon of 'local hopping'.[18] The insertion sites have been made publically available by submission to both the Retrovirus Tagged Cancer Gene Database (RTCGD; http://rtcgd.ncifcrf.gov/) and the Insertional Mutagenesis Database (http://imdb.nki.nl/).

Results

Generation of ETV6-RUNX1 mice

The endogenous *Etv6* locus was targeted to introduce a *Lox66/Lox71*-flanked cassette containing a splice acceptor (SA), exons 1-6 of human *RUNX1*, an IRES, a hyperactive variant of the *Sleeping Beauty* (*SB*) transposase (HSB5), and an FRT flanked PGK-*PuroΔ TK* drug selection marker into *Etv6* intron 5, as shown in Figure 1A. The targeting vector was introduced into ES cells and correctly targeted clones, $Etv6^{+/RUNX1}$ (ER), were identified by Southern blotting using a 5′ and 3′ external probe on *Stu*I-digested genomic DNA (Figure 1B). These ES cell clones were used to generate chimeric mice that transmitted the mutated allele through the germline. All offspring were genotyped by PCR to detect the presence of the transposase. The *PuroΔ TK* drug marker was removed by breeding the mice to a *Flpe*-deleter strain (FLPeR mice)[22] prior to tumor watch experiments.

RT-PCR performed on ER bone marrow cDNA confirmed the presence of the fusion transcript (not seen in $Etv6^{+/+}$ (wildtype) bone marrow cDNA; Figure 1C). Sequencing the RT-PCR product confirmed faithful splicing of the *Etv6* and *RUNX1* transcripts to produce an in-frame fusion transcript (Figure 1C). Quantitative-RT-PCR performed on RNA extracted from bone marrow, spleen and thymus showed that the relative expression level of the wildtype *Etv6* gene to be comparable between wildtype and ER mice, whereas the relative expression level of the *ETV6-RUNX1* fusion transcript was less than that of the wildtype *Etv6* transcript in ER tissues (Figure 1D). Immunoprecipitation followed by Western blot analysis confirmed the presence of the fusion protein (Figure S1).

ETV6-RUNX1 in embryonic development

Mice heterozygous for the *ETV6-RUNX1* allele (*EV*) were grossly normal at birth and fertile (data not shown). However, homozygosity resulted in embryonic lethality at day E10.5 (Figure S2A), similar to that seen in homozygous null *Etv6* mice ($Etv6^{-/-}$).[23] This result confirms that our *ETV6-RUNX1* allele does not produce a functional *ETV6* transcript. This is important when modeling human leukemia, as loss of the second *ETV6* allele is one of the most common genetic alterations in *ETV6-RUNX1* ALL patients.[7, 24]

These studies were performed using ER mice on a mixed genetic background (129;C57), and intercrossing of ER mice resulted in 54 of the 94 (57%) offspring being *TA*, which is within normal Mendelian ratios for homozygous lethal alleles (P=0.2285; Chi-squared test, 2-tailed). This suggests that *ETV6-RUNX1* does not have a dominant negative function over the remaining fusion partner alleles during embryogenesis, unlike the *RUNX1-RUNX1T1* fusion.[9] However, when the proportion of C57 genetic background was increased by breeding, ER mice were produced at sub-Mendelian ratios (Figure S2B) – a phenotype similar to that observed in a recently described conditional knockin *ETV6-RUNX1* mouse generated on a C57 background,[14] suggesting the C57 strain may contain a genetic modifier of the function of *ETV6-RUNX1* in embryonic development.

ETV6-RUNX1 expression predisposes to hematologic malignancies

Consistent with previous reports that *ETV6-RUNX1* expression does not grossly affect hematopoiesis in the post-natal period,[14] we did not observe significant gross perturbation of hematopoietic homeostasis in *ETV6-RUNX1* mice (as assessed by immunophenotyping of bone marrow at 3, 6 and 12 months of age; Figure S3). To model the 'second hit' event(s) that occurs in *ETV6-RUNX1* patients facilitating the development of overt leukemia, we intercrossed *ETV6-RUNX1* ($Etv6^{+/RUNX1}$; *ER*) mice with mice carrying the *T2Onc* transposon array ($T2Onc^{+/Tg}$).[18] To confirm that the *SB* system was functioning in these mice we firstly analyzed bone marrow cell lysates for the presence of SB transposase protein. Western blotting of these lysates using an anti-SB transposase antibody showed the presence of a 40 kDa band in mice carrying the *Etv6-RUNX1* allele, consistent with the molecular weight of the SB transposase (Figure 2A). Secondly, we performed 'excision PCR' on genomic tail DNA from the offspring (Figure 2B). A small PCR product (~200 bp) is only present in mice carrying both the transposon and transposase ($Etv6^{+/RUNX1}$; $T2Onc^{+/Tg}$, hereafter referred to as *EROnc* mice), indicative of 'jumping' of single transposons out of the array (into the genome) whereas mice carrying the transposon array alone ($Etv6^{+/+}$; $T2Onc^{+/Tg}$, hereafter referred to as *Onc* mice) show only a large PCR product (~2 kb) representing the transposon concatamer.

Mice of all four genotypes that arose from the intercrossing of $Etv6^{+/RUNX1}$ mice with $T2Onc^{+/Tg}$ mice: *EROnc* (n=90), $Etv6^{+/RUNX1}$; $T2Onc^{+/+}$ (hereafter refereed to as *ER*; n=54), *Onc* (n=50), and $Etv6^{+/+}$; $T2Onc^{+/+}$ (hereafter referred to as wildtype; n=22) were placed on tumor watch, and observed twice daily for signs of illness. Although mice of all genotypes developed hematological malignancies, *EROnc* mice showed a statistically significant increased incidence of leukemia and decreased survival compared with the other genotypes (P<0.0001; Figure 2C). ER mice (which carry the $Etv6^{RUNX1}$ allele without the *T2Onc* transposon allele, hence no mutagenesis) also showed decreased survival compared to *Onc* mice carrying just the *T2Onc* allele (i.e., no *Etv6-RUNX1* or transposase expression hence no mutagenesis).

This decreased survival in both cohorts was due to the development of hematological malignancies, which were classified according to the Bethesda criteria for murine malignancies using standard morphological, histological and immunophenotypic analysis

Europe PMC Funders Author Manuscripts

(Figure 2D).[25-26] Occasional mice (11/72 mice, 14%) in the *Onc* and *WT* cohorts presented with long latency predominantly T-cell acute leukemias. However the incidence of leukemia was significantly increased in the cohorts expressing *Etv6-RUNX1* (73/90 mice, 81% for the *EROnc* cohort and 16/54, 29% for *ER*). The presence of *Etv6-RUNX1* expression not only increased the incidence of acute leukemias, but also modulated the phenotype. In the *EROnc* cohort, acute myeloid leukemia (AML) predominated (34/73 cases, 46%), with T-cell ALL also seen (21/73, 28%). T-cell ALL predominated in the ER mice (11/16 cases, 68%), with an occasional case of AML seen. Importantly, 15 of 73 (21%) of *EROnc* mice developed B-cell precursor (BCP-ALL) as did a slightly smaller proportion of the ER cohort (2/16 cases, 13%). Most importantly, BCP-ALL was only seen in mice carrying the *ETV6-RUNX1* allele. This is the only mouse model of *ETV6-RUNX1* to develop BCP-ALL, either through spontaneous or mutagenesis-driven acquisition of 'second hits'.

ETV6-RUNX1-expressing mice develop a B-cell precursor acute lymphoblastic leukemia

Mice with the BCP-ALL phenotype demonstrated the obvious presence of lymphoblasts in the peripheral blood and bone marrow, and heavy infiltration of lymphoblasts in the spleen and liver, resulting in effacement of the normal cellular architecture and replacement with predominantly nucleolated blasts (Figure 3A). Immunophenotypic analysis of the bone marrow by FACS from the 17 cases of BCP-ALL showed the majority of tumors to be of early B cell progenitor immunophenotype ($B220^+$ $CD19^-$, IgM^-, IgD^-) (Figure 3B and S4). ETV6-RUNX1 patients typically have a surface phenotype reminiscent of pre-B cells (equivalent to Hardy Fraction C).[27] More detailed immunophenotyping of a subset of 7 cases predominantly showed a phenotypic profile ($AA4.1^+$, $CD24^+$, $CD43^+$, $BP1^-$, $IL7Ra^-$; Figure S4) consistent with early pro-B cells (Hardy Fraction B) suggesting transformation of a slightly earlier lymphoid progenitor. In addition, a number of cases also showed co-expression of myeloid ($Mac\text{-}1^+$) markers on lymphoblasts (Figure S4). Co-expression of myeloid antigens (particularly CD13 and CD33), is well described for patients with *ETV6-RUNX1* BCP-ALL.[27]

To further demonstrate clonality and determine the differentiation stage of the tumor the VDJ_H recombination status of three BCP-ALLs ($B220^+/CD19^-/sIg^-$ phenotype) was analyzed. Clonal DJ_H rearrangements were detected in two samples, however, both alleles were in germline configuration in the third (Figure 3C). Thus, taking into account the results of the IgH recombination and immunophenotyping analysis, these murine leukemias are B-cell precursor in origin, however, show an earlier arrest in B-cell ontogeny than typically found in *ETV6-RUNX1* BCP-ALL patients ($CD10^+/CD19^+$ and evidence of VDJ_H recombination).

Gene expression analysis to look at transcripts differentially expressed between BCP-ALL spleen and normal splenic tissue (*EROnc* mice with no disease, n=3), found statistically significant differential expression (typically down-regulation) of 125 genes ($P<0.05$; Table S1), several of which are known to be important for transition through pro-B and pre-B cell stages of development (including *Blk*, *Blnk*, *CD19*, *Ebf1*, *Foxo1*, *Irf4*, *Spib*, *Vpreb3i* and *Zhx2*.) Gene set enrichment analysis (GSEA) performed on these differentially expressed genes found the top 5 canonical pathways involved B-cell signalling or development (Table S2). There was also decreased expression of the chemokine receptors *Ccr6* (CD196) and *Cxcr5* (CD185), reported to be down-regulated in BCP-ALL patients.[28] Importantly, we also found decreased expression in genes found in deleted regions of human *ETV6-RUNX1* patients (including *Ebf1*, *Blnk*, and *Btg*)[7, 24] and decreased expression of *Ms4a1* (CD20), a B-lymphocyte surface antigen reported to be of lower expression in t(12;21)+ than t(12;21)− BCP-ALL cases.[29] Thus the molecular profiling of these leukemias in part mirrors human *ETV6-RUNX1* positive BCP-ALL.

Identification of co-operating mutations in ETV6-RUNX1-expressing mice using insertional mutagenesis

Genomic DNA extracted from leukemic tissue of 73 *Etv6*$^{+/RUNX1}$; *T2Onc*$^{+/Tg}$ (*EROnc*) mice was used in a splinkerette PCR reaction to produce barcoded PCR products that were subsequently pooled and directly sequenced on the 454 GS-FLX platform.[21] This generated 695,504 sequence reads, of which 51.5% unambiguously aligned to the mouse genome (see Figure S5). Using a previously developed computational pipeline to trim, map, and annotate each sequence read,[21] we were able to identify 23,529 unique (non-redundant) insertion sites. We used the Gaussian kernel convolution (GKC) algorithm to determine statistically significant common insertion sites (CIS; genomic regions with a higher density of insertion sites than expected by chance),[30] and CIS were assigned to genes as described previously.[21] In total, 71 leukemias (34 AML, 15 BCP-ALL, 19 T-ALL, 2 unclassified and 1 myeloproliferative) contributed to generate a total of 101 unique GKC CIS regions/genes, with an average of 15 ± 7 CIS/leukemia (listed in Figure 4 and Table S3). To identify potential co-occurring CIS and common patterns of mutation between each of the leukemias, a matrix of the leukemias against the unique CIS regions was constructed and hierarchical clustering performed to aggregate those with similar patterns of insertions (Figure 4). Interestingly, many of the CIS that were found in the BCP-ALLs were also found in the AML and T-ALLs (see Figure S6), suggesting that these CIS/genes may predispose to tumorigenesis in multiple hematopoietic lineages, or may affect HSC function before individual lineages are specified. However, the possibility cannot be excluded that since many of our BCP-ALLs also showed a population of cells with aberrant expression of myeloid markers (Mac-1 and Gr-1; Figures 3B and S4), mutation of genes involved in the myeloid pathway would be expected or that these tumors were polyclonal and contained a separate myeloid clone.

Restricting our analysis to the BCP-ALL cases (Table 1 and Figure S7), the most frequently targeted genes/loci were an intragenic region on mouse chromosome 7 (CIS peak location at 37320759), translation initiation factor 2 (*Eif2a*), the erythropoietin receptor (*Epor),* Ikaros family zinc finger 1 *(Ikzf1),* CCAAT/enhancer binding protein, alpha *(Cebpa*) and the cannabinoid receptor 2 (*Cnr2*). In some cases the transposons had inserted themselves in the forward orientation and were clustered in the non-coding introns upstream of the ATG start site, suggesting they act as activating mutations to induce over-expression of the gene (such as *Raf1* and *Mef2c*). In other cases, the transposons had inserted themselves in both the forward and reverse orientations and were scattered throughout the gene, suggesting they act as inactivating mutations, to produce a truncated transcript (such as *Ikzf1*). Although some of these genes/loci were also found as CIS in AML and T-ALL cases, 66% (22/33) of these CIS were exclusive to the BCP-ALL cases (including *Eif2a* and *Ikzf1*). Intriguingly, these B-cell specific genes did not appear to cluster together (Figure 4), suggesting that there is significant heterogeneity in the genes that can contribute to the development of acute lymphoblastic leukemia in this model.

Insertional mutagenesis in ETV6-RUNX1-expressing mice models human ALL

By performing cross-species comparisons we found an overlap between some of the CIS in our BCP-ALL cases and genes recurrently found to be altered in patients with *ETV6-RUNX1* positive ALL (Table 1), specifically insertions in the coding region of *Ikzf1* and *Epor*. *IKZF1* has a central role in the pathogenesis of BCP-ALL. Deletions involving *IKZF1* are common (30%) in high-risk/poor prognosis B-cell precursor ALL[31] (although not in *ETV6-RUNX1* ALL) and *EPOR* is consistently highly expressed in *ETV6-RUNX1* ALL.[32] Compared to control spleens (n=3), those spleens with insertions in *Epor* (n=2) showed a log-fold-change of 0.35 for *Epor* expression (which is ~27% increase in expression)[20] whereas those without insertions in *Epor* (n=13) showed a log-fold-change of −0.23 (which

is ~15% decrease in expression). This suggests that the insertions in the promoter region of *Epor* upregulate Epor expression, a finding consistent with *ETV6-RUNX1* ALL patients. In addition, we found *Met* to be a CIS, and c-MET activation specifically enhances FAS-mediated apoptosis in *ETV6-RUNX1* cells. Indeed, the c-MET/FAS complex is only found in normal B lymphocytes and *ETV6-RUNX1* leukemias and not B-ALLs that lack the t(12;21) translocation, an observation which may account for their high sensitivity to chemotherapeutic regimens.[33] We also found CIS in genes mutated in AML, specifically *Gata1* (*Gata-1* mutation is found in AMKL associated with Downs syndrome)[34] and *Cebpa* (mutations in *C/EBPA* are seen in AML).[35]

Seven of the CIS genes in our BCP-ALL samples had genomic locations syntenic with human chromosomal locations known to be regions of recurrent copy number change in *ETV6-RUNX1* patient samples, including *Fam46d*, *Gata1* and *L3mbtl3* (n ≥ 3/50 patients; Table 2). Although the genomic size of the lesions was quite large in some cases, it is possible that our CIS genes can serve as a focal point for identification of the causative gene in these regions.

Given the small number of BCP-ALL cases in this cohort (n=15), we were statistically underpowered to generate a large number of CIS. Therefore for the BCP-ALL cases we looked at the 4,787 unique/non-redundant insertion sites in addition to the CIS, and found that many of them were of interest because of their location relative to genes known to be dysregulated in *ETV6-RUNX1* positive ALL patients. These genes included *Lef1*, *Dpf3*, *Tbl1xr1*, *Ebf1* and *Nr3c1* (Table 3). Although the insertion frequency was too low, or the genomic distribution of the insertions too broad to be classified as a CIS, a frequency of 1-3 cases from a total of 15 represents 6-20%, and echoes the frequency reported in *ETV6-RUNX1* positive ALL patients.[7, 24]

Of particular importance was *Ebf1*. *EBF1* can activate expression of *PAX5*,[43] and analysis of cDNA from the 3 cases which carried *Ebf1* insertions showed splicing of *Ebf1* directly onto the splice acceptor/polyA of the transposon (Figure 5). This resulted in premature truncation of the gene at exon 6 and thus presumably an inability to activate Pax5. As well as *Ebf1*, we also had insertions in many other key regulators of B-cell development including *Ikzf1* (Figure S8), *Lef1*, *Tcf3* and *Blnk*, providing strong evidence that genetic alterations resulting in a block in B-lymphoid development are key events in the pathogenesis of B-ALL.

Discussion

ETV6-RUNX1 is the most common fusion oncogene associated with childhood ALL, and although generally associated with favorable prognosis, no faithful mouse models exist to provide mechanistic or potential therapeutic insights into this disease. Previous models have been hampered by potential overexpression of the fusion oncogene from transgenic or retroviral promoters, by a failure to generate leukemia or by generation of a leukemia of a differing phenotype.[10-14] In this report, we describe the generation of the first mouse model of *ETV6-RUNX1* that develops B-cell precursor (BCP)-ALL. In addition, through the use of the SB transposon system, we identify cooperating mutations that facilitate development of ALL, thus providing an excellent resource to further dissect the biology of this disease.

We identified a total of 102 unique statistically significant common insertion sites (CIS) regions/genes from the 71 leukemias analyzed (Table S3 and Figure 4). Interestingly, many of the CIS that were found in the BCP-ALLs (Table 1) were also found in the AML and T-ALL cases. Since expression of the fusion in our model occurs in hematopoietic stem cells (HSCs) following the expression pattern of endogenous *Etv6*, it likely that the fusion

'primes' cells to become leukemic with the actual phenotype driven by the nature of the cooperating mutations and the hematopoietic lineage/compartment in which they are acquired (before specification of the B-cell lineage). However, over-lapping CIS from the BCP-ALL and AML cases may reflect the fact that several of these BCP-ALL cases also expressed myeloid markers (Figure S4), as the co-expression of myeloid antigens has been described in ETV6-RUNX1 positive ALL patients.[27]

Cross-species analysis of the BCP-ALL cases identified insertions/CIS in genes known to be dysregulated in human *ETV6-RUNX1* positive ALL patients, including *Btg1, Dpf3, Ebf1, Epor, Fhit, Grik2, Ikzf1, Lef1, Mllt3, Nf1, Nr3c1/2, Rap1b, Rb1, Tbl1xr1, Tcf12* and *Zcchc7* (Table 3). Previous studies that have performed genome-wide profiling of genetic alterations in *ETV6-RUNX1* BCP-ALL have shown that although a small number of mutations predominate, the mutational spectrum is highly heterogeneous, with numerous recurrent lesions generating mutations or copy number alterations in only a few patients.[7, 41] For example, in 47 cases of *ETV6-RUNX1* positive ALL, deletions at chromosome 12p13.2 (*ETV6*) and 9p13.2 (*PAX5*) were found in as many as 33 and 13 patients (70% and 27% of cases) respectively. However, the majority of chromosomal gains/losses were found in less than eight (14%) patients, including deletions at 3q26.32 (*TBL1XR1*), 5q33.3 (*EBF1*) and 5q31.3 (*NR3C1*), with 8 of the genomic rearrangements only being found in 1 (2%) patient, including deletions at 4q25 (*LEF1*), 10q24.1 (*BLNK*) and 14q24.2 (*DPF3*).[7] Thus although our insertions in these genes do not classify as "CIS", a 'hit' frequency of 6-20% echoes the 2-14% frequency reported in *ETV6-RUNX1* positive ALL patients.

In addition, it is interesting that some genes in recurrent regions of chromosomal imbalance were not involved, including *Etv6*, *Cdkn2a/Cdkn2b* (encoding *Ink4a/Arf*) and *Pax5*.[7, 24] This could be due to our small sample size of 15 BCP-ALL cases. Alternatively, it is possible that these genes were not available for insertion, through prior inactivation by other means such as focal deletion or point mutation (potentially through illegitimate RAG-mediated recombination). It is also recognized that the mutation mechanism itself can contribute to (bias) the selection of target genes. For example, AID expression in CML cells has been suggested to promote overall genetic instability by hypermutation of tumor suppressor and DNA repair genes.[44] Moreover, malignancies of progenitor B-cells have also been associated with aberrant RAG mediated recombination.[45] Both of these mechanisms are sequence specific and may contribute a different bias to our experimental system in the selection of specific targets. Finally it is also possible that this reflects the fact that our disease involves an earlier cell type (pro-B) than typically seen in *ETV6-RUNX1* positive ALL patients (which are typically pre-B).

However, although *Pax5* was not involved in our screen, we identified mutations in *Ebf1* and *Tcf3* (*E2A*), which cooperatively regulate *PAX5*,[46] and *Tcf4*, *Lef1*, and *CD44*, which are PAX5-activated genes.[47-48] These "complementary" lesions therefore potentially having the same signaling impact as if we had directly mutated *Pax5*. Interestingly, a study recently found that many PAX5-regulated genes lie within 100 kb of an EBF1-bound region, suggesting coordinated regulation of common target genes by these transcription factors.[49]

Of the CIS regions/genes that were identified in the BCP-ALLs (Table 1), *Epor* and *Met* are known to show altered expression in *ETV6-RUNX1* positive ALL patients (and *Ikzf* in some cases). Although the other regions/genes have not been associated with *ETV6-RUNX1* ALL, some have been shown to play a role in lymphocyte biology. For example, *Cebpa* belongs to the *CEBP* family, which have recently been found to show dysregulated expression in B-cell precursors and can contribute to their malignant transformation[50] and *Rasgrf1* has been shown to be over-expressed in B-cell chronic lymphocytic leukemia (B-CLL) compared to normal B lymphocytes.[51] Other regions/genes have previously been

Europe PMC Funders Author Manuscripts

implicated as players in tumorigenesis, such as *Cnr2*, a proto-oncogene that has been postulated to offer a growth advantage in leukemia cells[52] and *Psd3*, reduced expression of which is believed to contribute to malignant progression.[53] Thus these genes are all attractive candidates to co-operate with *ETV6-RUNX1* in promoting ALL, and as new technologies emerge that allow further interrogation of cancer biology (such as RNA sequencing, exome sequencing, etc) new genes will constantly be added to the list of those found to be dysregulated in *ETV6-RUNX1* ALL.

In summary, we present the first mouse model of *ETV6-RUNX1* that exhibits BCP-ALL. This model will prove a valuable resource to both further understanding of the disease and in the development of therapeutics in *ETV6-RUNX1* positive ALL.

Supplementary Material

Refer to Web version on PubMed Central for supplementary material.

Acknowledgments

The authors wish to thank the staff of the Research Support Facility at the Wellcome Trust Sanger Institute for looking after the mice and Mahrokh Nohadani for performing the immunohistochemistry. LvdW is supported by a Fellowship from the Kay Kendall Leukemia Fund. DJA is supported by Cancer Research-UK and the Wellcome Trust. BJH and GG are supported by an MRC-UK Senior Fellowship (BJH) and Cancer Research-UK. FWvD and MG are supported by the Kay Kendall Leukaemia Fund and Leukaemia & Lymphoma Research UK. AEC and LSM are supported by the BBSRC. CGM is supported by the American Lebanese Syrian Associated Charities of St Jude Children's Research Hospital, and is a Pew Scholar in the Biomedical Sciences.

References

1. Romana SP, Mauchauffé M, Le Coniat M, et al. The t(12;21) of acute lymphoblastic leukemia results in a TEL-AML1 gene fusion. Blood. 1995; 85:3662–3670. [PubMed: 7780150]
2. Shurtleff SA, Buijs A, Behm FG, et al. TEL/AML1 fusion resulting from a cryptic t(12;21) is the most common genetic lesion in pediatric ALL and defines a subgroup of patients with an excellent prognosis. Leukemia. 1995; 9:1985–1989. [PubMed: 8609706]
3. Greaves MF, Wiemels J. Origins of chromosome translocations in childhood leukaemia. Nat Rev Cancer. 2003; 3:639–649. [PubMed: 12951583]
4. Hong D, Gupta R, Ancliff P, et al. Initiating and cancer-propagating cells in TEL-AML1-associated childhood leukemia. Science. 2008; 319:336–339. [PubMed: 18202291]
5. Castor A, Nilsson L, Astrand-Grundström I, et al. Distinct patterns of hematopoietic stem cell involvement in acute lymphoblastic leukemia. Nat Med. 2005; 11:630–637. [PubMed: 15908956]
6. Mori H, Colman SM, Xiao Z, et al. Chromosome translocations and covert leukemic clones are generated during normal fetal development. Proc Natl Acad Sci USA. 2002; 99:8242–8247. [PubMed: 12048236]
7. Mullighan CG, Goorha S, Radtke I, et al. Genome-wide analysis of genetic alterations in acute lymphoblastic leukaemia. Nature. 2007; 446:758–764. [PubMed: 17344859]
8. Bateman CM, Colman SM, Chaplin T, et al. Acquisition of genome-wide copy number alterations in monozygotic twins with acute lymphoblastic leukemia. Blood. 2010; 115:3553–3558. [PubMed: 20061556]
9. Higuchi M, O'Brien D, Kumaravelu P, Lenny N, Yeoh EJ, Downing JR. Expression of a conditional AML1-ETO oncogene bypasses embryonic lethality and establishes a murine model of human t(8;21) acute myeloid leukemia. Cancer Cell. 2002; 1:63–74. [PubMed: 12086889]
10. Bernardin F, Yang Y, Cleaves R, et al. TEL-AML1, expressed from t(12;21) in human acute lymphocytic leukemia, induces acute leukemia in mice. Cancer Res. 2002; 62:3904–3908. [PubMed: 12124316]
11. Tsuzuki S, Seto M, Greaves M, Enver T. Modeling first-hit functions of the t(12;21) TEL-AML1 translocation in mice. Proc Natl Acad Sci U S A. 2004; 101:8443–8448. [PubMed: 15155899]

12. Fischer M, Schwieger M, Horn S, et al. Defining the oncogenic function of the TEL/AML1 (ETV6/RUNX1) fusion protein in a mouse model. Oncogene. 2005; 24:7579–7591. [PubMed: 16044150]
13. Sabaawy HE, Azuma M, Embree LJ, Tsai HJ, Starost MF, Hickstein DD. TEL-AML1 transgenic zebrafish model of precursor B cell acute lymphoblastic leukemia. Proc Natl Acad Sci U S A. 2006; 103:15166–15171. [PubMed: 17015828]
14. Schindler JW, Van Buren D, Foudi A, et al. TEL-AML1 corrupts hematopoietic stem cells to persist in the bone marrow and initiate leukemia. Cell Stem Cell. 2009; 5:43–53. [PubMed: 19570513]
15. Yant SR, Huang Y, Akache B, Kay MA. Site-directed transposon integration in human cells. Nucleic Acids Res. 2007; 35:e50. [PubMed: 17344320]
16. van der Weyden L, Adams DJ, Harris LW, Tannahill D, Arends MJ, Bradley A. Null and conditional semaphorin 3B alleles using a flexible puroDeltatk loxP/FRT vector. Genesis. 2005; 41:171–178. [PubMed: 15789413]
17. Morrow M, Samanta A, Kioussis D, Brady HJ, Williams O. TEL-AML1 preleukemic activity requires the DNA binding domain of AML1 and the dimerization and corepressor binding domains of TEL. Oncogene. 2007; 26:4404–4414. [PubMed: 17237815]
18. Collier LS, Carlson CM, Ravimohan S, Dupuy AJ, Largaespada DA. Cancer gene discovery in solid tumours using transposon-based somatic mutagenesis in the mouse. Nature. 2005; 436:272–276. [PubMed: 16015333]
19. Yang YH, Dudoit S, Luu P, et al. Normalization for cDNA microarray data: a robust composite method addressing single and multiple slide systematic variation. Nucleic Acids Res. 2002; 30:e15. [PubMed: 11842121]
20. Benjamini Y, Hochberg Y. Controlling the false discovery rate: a practical and powerful approach to multiple testing. J Roy Statist Soc Ser B. 1995; 57:289–300.
21. March HN, Rust AG, Wright NA, et al. Insertional mutagenesis reveals multiple networks of co-operating genes driving intestinal mutagenesis. Submitted to Nature Genetics. Jul.2010 Manuscript ID: NG-A28875.
22. Farley FW, Soriano P, Steffen LS, Dymecki SM. Widespread recombinase expression using FLPeR (flipper) mice. Genesis. 2000; 28:106–110. [PubMed: 11105051]
23. Wang LC, Kuo F, Fujiwara Y, Gilliland DG, Golub TR, Orkin SH. Yolk sac angiogenic defect and intra-embryonic apoptosis in mice lacking the Ets-related factor TEL. EMBO J. 1997; 16:4374–4383. [PubMed: 9250681]
24. Tsuzuki S, Karnan S, Horibe K, et al. Genetic abnormalities involved in t(12;21) TEL-AML1 acute lymphoblastic leukemia: analysis by means of array-based comparative genomic hybridization. Cancer Sci. 2007; 98:698–706. [PubMed: 17374122]
25. Morse HC 3rd, Anver MR, Fredrickson TN, et al. Bethesda proposals for classification of lymphoid neoplasms in mice. Blood. 2002; 100:246–58. [PubMed: 12070034]
26. Kogan SC, Ward JM, Anver MR, et al. Bethesda proposals for classification of nonlymphoid hematopoietic neoplasms in mice. Blood. 2002; 100:238–245. [PubMed: 12070033]
27. Romana SP, Poirel H, Leconiat M, et al. High frequency of t(12;21) in childhood B-lineage acute lymphoblastic leukemia. Blood. 1995; 86:4263–4269. [PubMed: 7492786]
28. Wong S, Fulcher D. Chemokine receptor expression in B-cell lymphoproliferative disorders. Leuk Lymphoma. 2004; 45:2491–2496. [PubMed: 15621766]
29. De Zen L, Orfao A, Cazzaniga G, et al. Quantitative multiparametric immunophenotyping in acute lymphoblastic leukemia: correlation with specific genotype. I. TEL/AML1 ALLs identification. Leukemia. 2000; 14:1225–1231. [PubMed: 10914546]
30. de Ridder J, Uren A, Kool J, Reinders M, Wessels L. Detecting statistically significant common insertion sites in retroviral insertional mutagenesis screens. PLoS Comput Biol. 2006; 2:e166. [PubMed: 17154714]
31. Mullighan CG, Su X, Zhang J, et al. Deletion of IKZF1 and prognosis in acute lymphoblastic leukemia. N. Engl. J. Med. 2009; 360:470–480. [PubMed: 19129520]

32. Fine BM, Stanulla M, Schrappe M, Ho M, Viehmann S, Harbott J, Boxer LM. Gene expression patterns associated with recurrent chromosomal translocations in acute lymphoblastic leukemia. Blood. 2004; 103:1043–1049. [PubMed: 14525776]
33. Accordi B, Pillozzi S, Dell'Orto MC, et al. Hepatocyte growth factor receptor c-MET is associated with FAS and when activated enhances drug-induced apoptosis in pediatric B acute lymphoblastic leukemia with TEL-AML1 translocation. J Biol Chem. 2007; 282:29384–29393. [PubMed: 17673463]
34. Wechsler J, Greene M, McDevitt MA, et al. Acquired mutations in GATA1 in the megakaryoblastic leukemia of Down syndrome. Nat Genet. 2002; 32:148–152. [PubMed: 12172547]
35. Lu Y, Chen W, Chen W, Stein A, Weiss LM, Huang Q. C/EBPA gene mutation and C/EBPA promoter hypermethylation in acute myeloid leukemia with normal cytogenetics. Am J Hematol. 2010; 85:426–430. [PubMed: 20513120]
36. Kuiper RP, Schoenmakers EF, van Reijmersdal SV, et al. High-resolution genomic profiling of childhood ALL reveals novel recurrent genetic lesions affecting pathways involved in lymphocyte differentiation and cell cycle progression. Leukemia. 2007; 21:1258–1266. [PubMed: 17443227]
37. Yeoh EJ, Ross ME, Shurtleff SA, et al. Classification, subtype discovery, and prediction of outcome in pediatric acute lymphoblastic leukemia by gene expression profiling. Cancer Cell. 2002; 1:133–143. [PubMed: 12086872]
38. Ross ME, Zhou X, Song G. Classification of pediatric acute lymphoblastic leukemia by gene expression profiling. Blood. 2003; 102:2951–2959. [PubMed: 12730115]
39. Fine BM, Stanulla M, Schrappe M. Gene expression patterns associated with recurrent chromosomal translocations in acute lymphoblastic leukemia. Blood. 2004; 103:1043–1049. [PubMed: 14525776]
40. Armstrong SA, Mabon ME, Silverman LB. FLT3 mutations in childhood acute lymphoblastic leukemia. Blood. 2004; 103:3544–3546. [PubMed: 14670924]
41. Lilljebjörn H, Soneson C, Andersson A. The correlation pattern of acquired copy number changes in 164 ETV6/RUNX1-positive childhood acute lymphoblastic leukemias. Hum Mol Genet. 2010; 19:3150–3158. [PubMed: 20513752]
42. Mullighan CG, Phillips LA, Su X. Genomic analysis of the clonal origins of relapsed acute lymphoblastic leukemia. Science. 2008; 322:1377–1380. [PubMed: 19039135]
43. Zandi S, Mansson R, Tsapogas P, Zetterblad J, Bryder D, Sigvardsson M. EBF1 is essential for B-lineage priming and establishment of a transcription factor network in common lymphoid progenitors. J Immunol. 2008; 181:3364–3372. [PubMed: 18714008]
44. Klemm L, Duy C, Iacobucci I, Kuchen S, von Levetzow G, Feldhahn N, Henke N, Li Z, Hoffmann TK, Kim YM, Hofmann WK, Jumaa H, Groffen J, Heisterkamp N, Martinelli G, Lieber MR, Casellas R, Müschen M. The B cell mutator AID promotes B lymphoid blast crisis and drug resistance in chronic myeloid leukemia. Cancer Cell. 2009; 16:232–245. [PubMed: 19732723]
45. Tsai AG, Lu H, Raghavan SC, Muschen M, Hsieh CL, Lieber MR. Human chromosomal translocations at CpG sites and a theoretical basis for their lineage and stage specificity. Cell. 2008; 135:1130–1142. [PubMed: 19070581]
46. Busslinger M. Transcriptional control of early B cell development. Annu Rev Immunol. 2004; 22:55–7. [PubMed: 15032574]
47. Pridans C, Holmes ML, Polli M. Identification of Pax5 target genes in early B cell differentiation. J Immunol. 2008; 180:1719–1728. [PubMed: 18209069]
48. Schebesta A, McManus S, Salvagiotto G, Delogu A, Busslinger GA, Busslinger M. Transcription factor Pax5 activates the chromatin of key genes involved in B cell signaling, adhesion, migration, and immune function. Immunity. 2007; 27:49–63. [PubMed: 17658281]
49. Treiber T, Mandel EM, Pott S, Györy I, Firner S, Liu ET, Grosschedl R. Early B cell factor 1 regulates B cell gene networks by activation, repression, and transcription-independent poising of chromatin. Immunity. 2010; 32:714–725. [PubMed: 20451411]
50. Akasaka T, Balasas T, Russell LJ. Five members of the CEBP transcription factor family are targeted by recurrent IGH translocations in B-cell precursor acute lymphoblastic leukemia (BCP-ALL). Blood. 2007; 109:3451–3461. [PubMed: 17170124]

51. Jelinek DF, Tschumper RC, Stolovitzky GA. Identification of a global gene expression signature of B-chronic lymphocytic leukemia. Mol Cancer Res. 2003; 1:346–361. [PubMed: 12651908]
52. Valk PJ, Delwel R. The peripheral cannabinoid receptor, Cb2, in retrovirally-induced leukemic transformation and normal hematopoiesis. Leuk Lymphoma. 1998; 32:29–43. [PubMed: 10036999]
53. van den Boom J, Wolter M, Blaschke B, Knobbe CB, Reifenberger G. Identification of novel genes associated with astrocytoma progression using suppression subtractive hybridization and real-time reverse transcription-polymerase chain reaction. Int J Cancer. 2006; 119:2330–2338. [PubMed: 16865689]

Europe PMC Funders Author Manuscripts

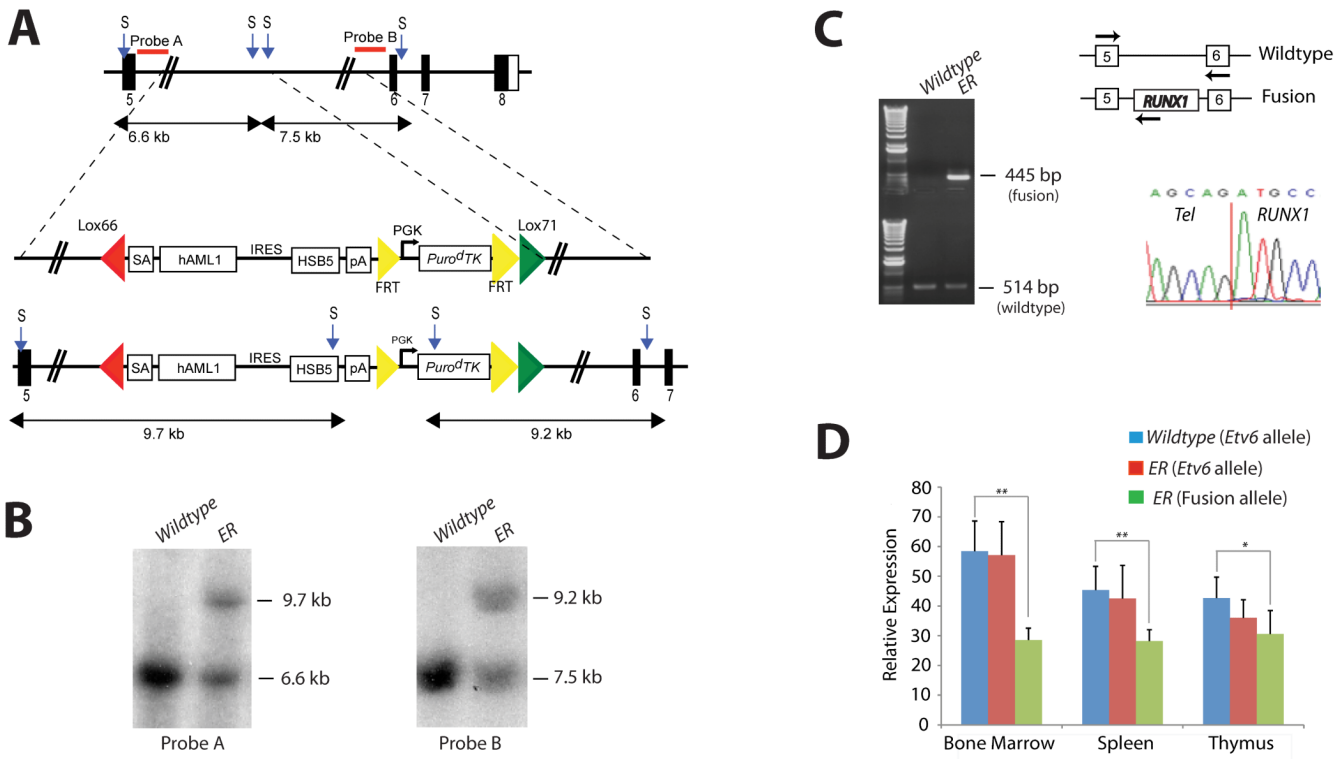

Figure 1. Generation of the *Etv6-RUNX1* transposase knockin allele (*Etv6*$^{+/RUNX1}$)

A. The endogenous *Etv6* locus was targeted to introduce a splice acceptor (SA), exons 1-6 of human *RUNX1*, an *IRES* followed by a hyperactive variant of the *Sleeping Beauty* transposase (HSB5), and an *FRT*-flanked *PGK-Puro*^{d}*TK* drug selection marker between exons 5 and 6. The entire cassette was flanked by *Lox66* and *Lox71* sites for potential Cre-mediated inactivation of the *Etv6-RUNX1* fusion gene. The *Puro*^{d}*TK* drug marker was removed by breeding mice to a Flpe deleter strain prior to tumor watch experiments. Probe A (5′) and Probe B (3′) are shown. S, *Stu*I. **B.** Southern blot analysis on *Stu*I digested tail DNA confirmed germline transmission and homologous recombination of the 5′ and 3′ targeting vector arms. **C.** RT-PCR showing expression of *Etv6-RUNX1* fusion transcripts in bone marrow from *Etv6*$^{+/RUNX1}$ mice, using primers located as indicated by the arrows on the schematic of the *Etv6* locus. Lower panel shows a sequence trace showing splicing of the *Etv6* and *RUNX1* transcripts to produce an in-frame fusion transcript. **D.** qPCR of *Etv6* and *Etv6-RUNX1* fusion transcripts (using primers as mentioned above). RNA was extracted from bone marrow, spleen and thymus. Relative *Etv6* gene expression in wildtype (blue) and *Etv6*$^{+/RUNX1}$ tissues (red), and relative *Etv6-RUNX1* fusion transcript expression in *Etv6*$^{+/RUNX1}$ tissues (green) is shown. The data was collected from the analysis of 5 littermate mice of each genotype (±SD). ** P<0.005, * P<0.05.

Europe PMC Funders Author Manuscripts

Europe PMC Funders Author Manuscripts

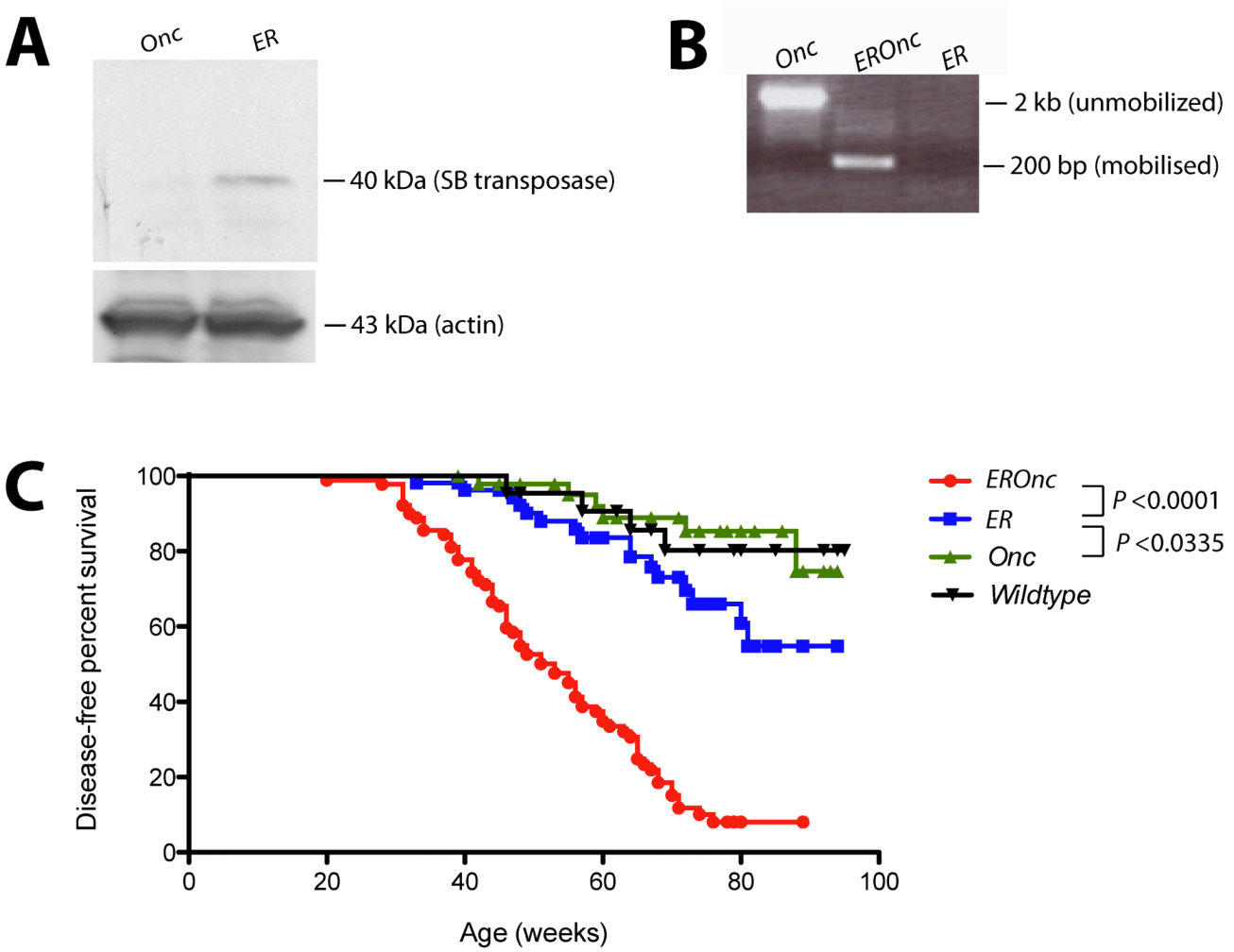

D

Category	*ERONc*	*ER*	*Onc*	*Wildtype*
Acute leukaemia - precursor T (T-ALL)	21	11	6	2
Acute leukaemia - myeloid with maturation (AML)	34	2	1	0
Acute leukaemia - precursor B (BCP-ALL)	15	2	0	0
Acute leukaemia - unclassified	2	0	0	2
Myeloproliferative disease	1	1	0	0
Total	73	16	7	4

Figure 2. Activation of transposon mutagenesis in *Etv6*$^{+/RUNX1}$ mice

A. Western blot showing expression of the *Sleeping Beauty* transposase in the bone marrow of *Etv6*$^{+/RUNX1}$ (*ER*) mice, but not mice carrying the *T2Onc* transposon (*Onc*). **B**. 'Excision' PCR showing mobilization of the transposon in bone marrow from *Etv6*$^{+/RUNX1}$; *T2Onc*$^{+/Tg}$ (*ERONc*) mice, as evidenced by the 200 bp 'excision' band (instead of the 2 kb band seen in mice carrying the unmobilized transposon array, i.e., *Etv6*$^{+/+}$; *T2Onc*$^{+/Tg}$ (*Onc*) mice). **C**. Kaplan-Meier curves showing the tumor latency of 'jumping' *Etv6*$^{+/RUNX1}$; *T2Onc*$^{+/Tg}$ (*ERONc*) mice and 'non-jumping' control mice (*ER*, *Onc* and wildtype). **D**. Categorization of the malignancies developed by mice shown in the Kaplan-Meier curve

according to the Bethesda criteria for lymphoid and non-lymphoid murine malignancies.[25-26]

Europe PMC Funders Author Manuscripts

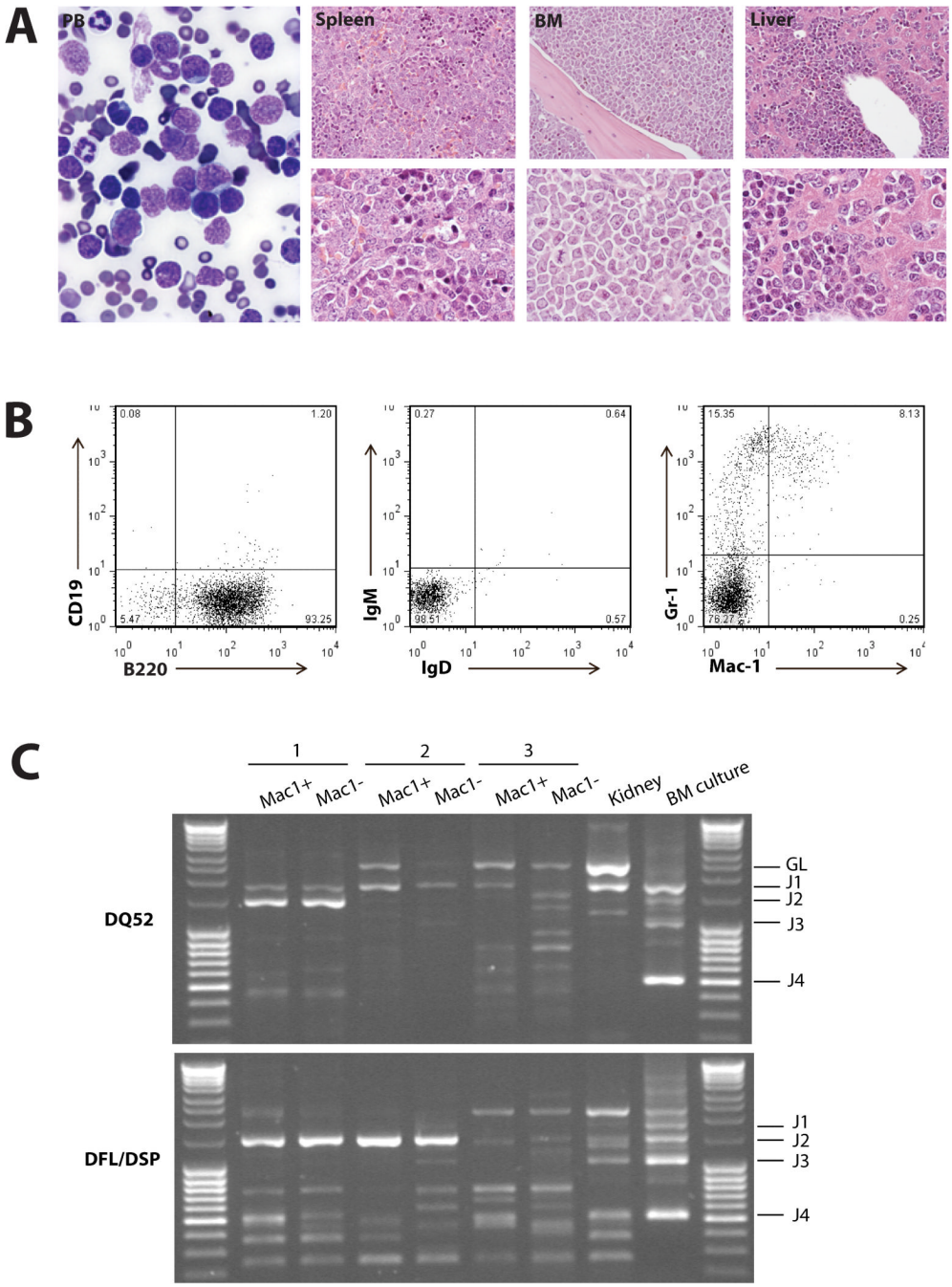

Figure 3. *Etv6*$^{+/}$*RUNX1* mice with 'second hits' develop a pre-B acute lymphoblastic leukemia recapitulating features of the human disease

A. Peripheral blood (PB; ×2000 magnification), spleen, bone marrow and liver (×400 magnification in upper panels and ×1000 magnification in lower panels) from a representative mouse with BCP-ALL. The presence of lymphoblasts in the peripheral blood is obvious, as is the infiltration of the spleen, bone marrow and liver (2nd-4th panels), with effacement of the normal cellular architecture and replacement by nucleolated blasts. **B.** FACS plots from the bone marrow of a representative mouse demonstrate only background Gr-1/Mac1 myeloid cells, with the majority of cells having a B220^{+}/CD19^{-}/sIg- phenotype in keeping with BCP-ALL. **C.** D-J PCR rearrangement studies (involving DQ52 and DFL/

Europe PMC Funders Author Manuscripts

DSP genes) were performed on spleen or bone marrow gDNA of three mice with phenotypic B-ALL. Negative control was gDNA from C57BL/6J mouse kidney (known to be unrearranged), and positive control was gDNA from a C57BL/6J primary pro-B cell bone marrow culture (known to contain a lot of DJ-rearranged alleles). Sample 1 shows two different rearrangement events (DQ52-J2 and DFL/DSP-J2 rearrangements), in keeping with a clonal B-cell population with both alleles D-J recombined. Sample 2 shows both a germline band and an identical DFL/DSP-J2 band, in keeping with a clonal B-cell population with rearrangement of one allele and germline configuration of the other. Sample 3 shows an absence of recombination.

Europe PMC Funders Author Manuscripts

Europe PMC Funders Author Manuscripts

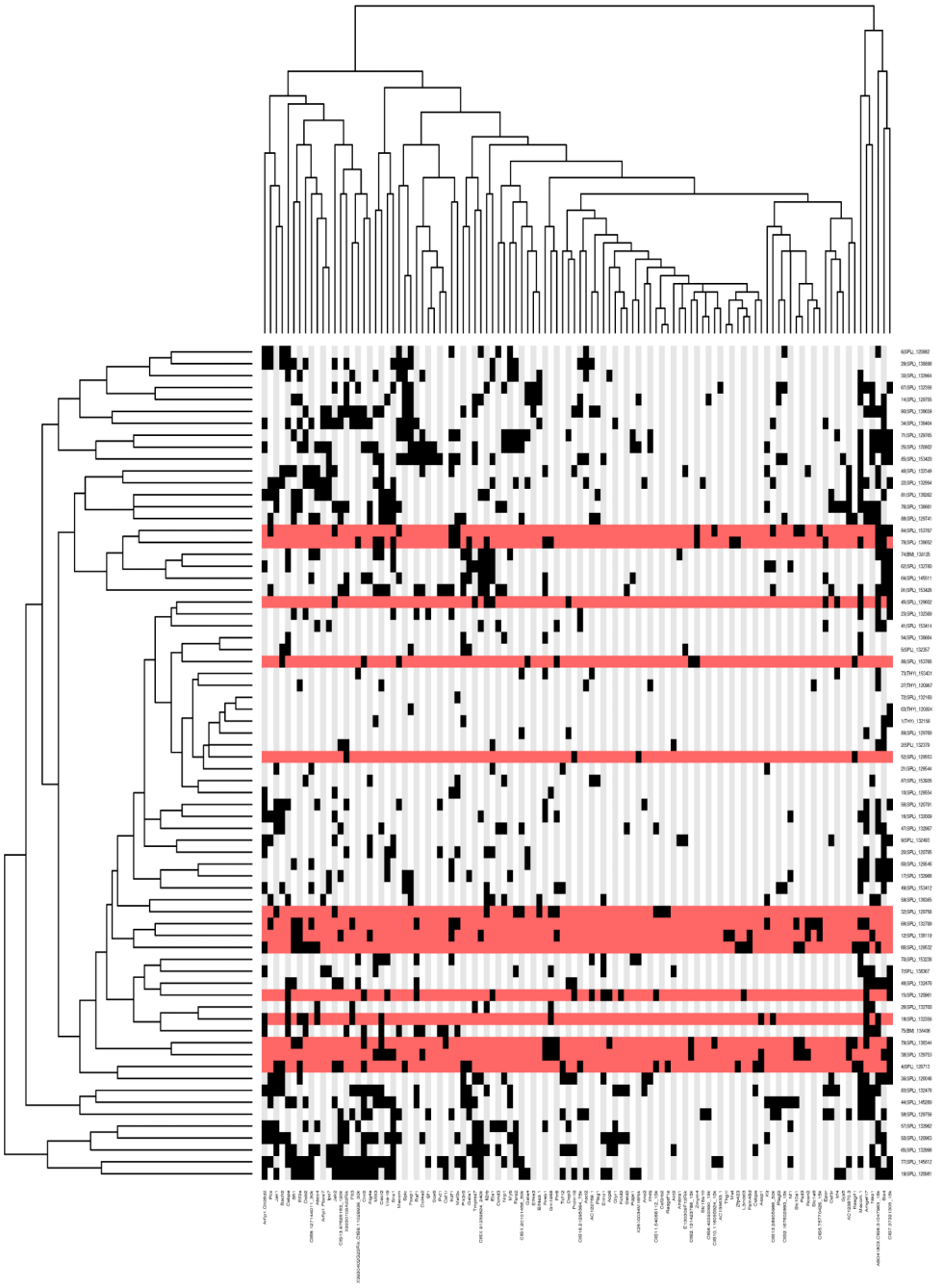

Figure 4. Hierarchical clustering of the leukemias and their mutated genes based on common insertion sites

A matrix of 71 leukemias against the 102 common insertion site (CIS) genes identified by analysis of transposon insertions by the Gaussian kernel convolution method was constructed. Although 73 leukemias were subjected to LM-PCR, sample 120992 did not have any insertions that were mapped and sample 138641 had only 44 insertions sites that were mapped but none of these contributed to any CIS, thus these two samples do not appear in the heatmap as the heatmap is based on the co-occurrence of insertions in CIS. Hierarchical clustering was performed on a binarized version of the matrix using the Hamming distance metric along both the rows and columns, to aggregate leukemias and CIS

genes with similar insertions patterns. The two resulting dendrograms were visualized as a heatmap, where black squares indicate the presence of at least one insertion in the tumor, and grey no insertion site. Leukemia rows highlighted in red indicate a BCP-ALL phenotype (n=15; only 14 rows highlighted in red because no insertions were found in the called CIS for sample 138895). The clustering and visualization were performed using the R programming language (version 2.10.0) and Bioconductor (version 2.5).

Europe PMC Funders Author Manuscripts

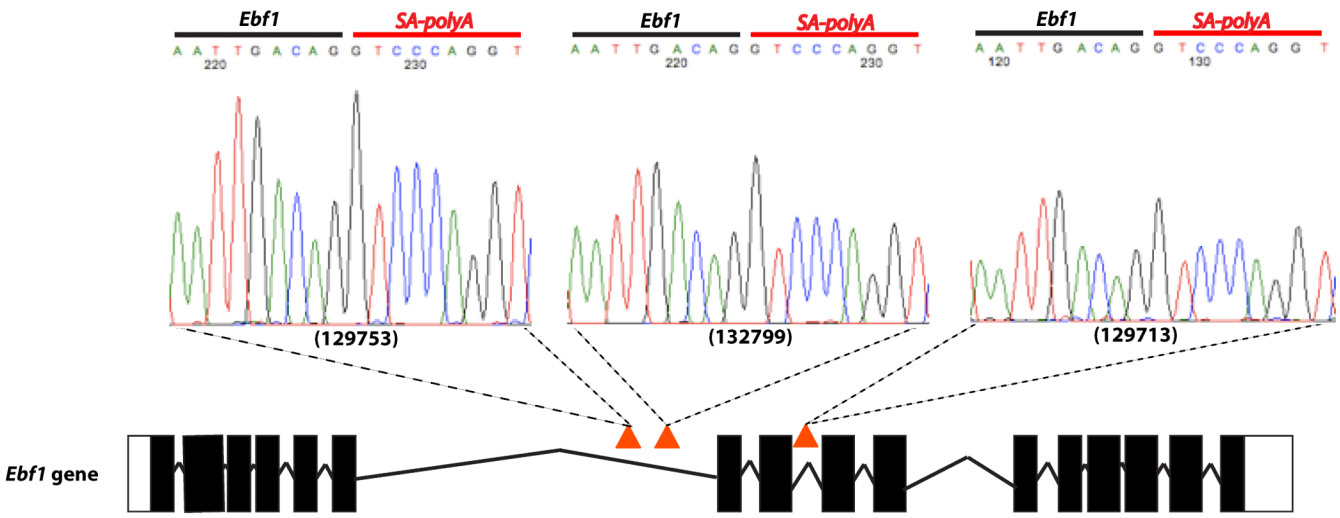

Figure 5. Insertions in the *Ebf1* gene

Three *Etv6*$^{+/RUNX1}$; *T2Onc*$^{+/Tg}$ (*EROnc*) mice (129753, 132799 and 129713) that developed BCP-ALL carried insertions in the *Ebf1* gene (indicated by the red triangles in introns 6 and 8). Sequencing of the insertion-genome junction from splenic cDNA of these mice showed the splicing of *Ebf1* directly onto the splice acceptor (SA)-polyA from the transposon. Although sample 129713 carried an insertion in intron 8, we detected splicing onto the transposon directly from exon 6.

Europe PMC Funders Author Manuscripts

Table 1

Gaussian kernel convolution (GKC) common insertion sites (CIS) identified in all B-cell precursor acute lymphoblastic leukemia (BCP-ALL) cases

CIS shown in bold are only found in the BCP-ALLs (n=15), not the other ALL cases. CIS that are not located within ± 150K base pairs of a gene are given the label 'CIS' followed by the chromosome and the peak location of the Gaussian kernel.

Gene	Chr.	CIS leak location	GKC scale (Kbps)	Tumours with CIS	Unique insertions	Other genes in the CIS interval
CIS7:37320759	7	37320759	15	6	12	-
Eif2a	3	58350745	240	6	10	*2810407C02Rik, AC111080.1, AC119873.1, AC132302.1, AC142228.1, Commd2, Gm410, Pfn2, Rnf13, Serp1, Siah2, Tsc22d2, U6, Wwtr1*
Ikzf1	11	11652893	15	4	9	-
Epor	9	21769506	15	2	9	-
Cebpa	7	35899198	15	2	8	*5S_rRNA*
Cnr2	4	135467435	15	4	7	-
Prr8	5	28716988	75	5	6	*AC121843.1, AC134530.1, Shh*
Rcan2	17	44101905	75	3	6	*7SK, CT025668.2*
CIS6:31099937	6	31099937	30	5	5	*AB041803, AC153820.1/4, RP23-459L15.3*
Rasgrf1	9	89867811	15	5	5	-
Slc10a1	12	82095071	15	5	5	*Sfrs5*
Gm1968	16	29983555	30	5	5	*CT025592.1, CT030736.1*
Mecom	3	30047667	15	4	5	-
Psd3	8	70258943	30	4	5	*AC109142.1, AC109142.2*
Sfi1	11	3065855	50	4	5	*AL671968.1/2/4/5, Drg1, Eif4enif1*
CIS5:75770426	5	75770426	15	3	5	U6
Raf1	6	115605310	120	2	5	-
Kctd2	11	115288407	15	1	5	-
CIS11:54066112	11	54066112	15	3	4	*AL596103.1, Il3*
Asap1	15	64063966	30	3	4	-
Met	6	17424888	15	2	4	-
Fam46d	X	105018631	15	2	4	*2610002M06Rik*
Csf2rb2	15	78135922	15	1	4	-
CIS2:131423786	2	131423786	15	3	3	-
Zmym4	4	126594535	15	3	3	-

Europe PMC Funders Author Manuscripts

Gene	Chr.	CIS leak location	GKC scale (Kbps)	Tumours with CIS	Unique insertions	Other genes in the CIS interval
Zfp423	8	90421110	15	3	3	-
Mef2c	13	83672435	15	3	3	-
Il2rb	15	78328305	15	3	3	-
Rasgef1a	6	118007445	15	2	3	-
L3mbtl3	10	26098605	15	2	3	-
CIS10:116095924	10	116095924	15	2	3	-
Thg1l	11	45761354	15	1	3	-
Gata1	X	7537541	15	2	2	-

Table 2

CIS identified in the BCP-ALL samples whose homologous human chromosomal location was found to be a recurrent region of copy number (CN) change in human *ETV6-RUNX1* leukemias

A total of 50 *ETV6-RUNX1* patient samples were analyzed by SNP array, and the CN changes for the relevant lesions shown. Deletions correspond to CN<2 and amplifications to CN>2. The LiftOver tool (http://genome.ucsc.edu/cgi-bin/hgLiftOver) was used to find the associated human chromosomal region for each mouse CIS gene (using the GRCh37/hg19 assembly). Statistical significance for each CIS was calculated (using 1,000 randomly selected Refseq genes) and a cut-off of P<0.2 was used.

Mouse CIS (no. insertions)	Homologous human region (chr: basepair)	No. patients	CN changes in patient samples	CN lesion size (Mb): mean ± SD (median)
Fam46d (4)	X: 79589304-79616318	10	1.4, 1.34, 1.36, 1.28, 1.53, 1.11, 1, 2.99, 0.85, 1.23	124 ± 43 (150)
Gata1 (2)	X: 48645231-48659263	9	2.47, 1.34, 1.36, 1.28, 1.11, 1, 2.99, 0.85, 1.23	132 ± 34 (151)
L3mbtl3 (3)	6: 130336865-130339827	5	0.88, 1.28, 0.84, 1.55, 3.17	110 ± 57 (87)
CIS7:37320759 (12)	19: 31962394-32030766	3	1.68, 1.65, 1.06	23 ± 29 (7)
Cebpa (8)	19: 33765960-33835715	3	1.68, 1.65, 1.06	23 ± 29 (7)
Gm1968 (5)	3: 193728382-193781161	3	0.98, 0.94, 1.59	37 ± 42 (20)
Psd3 (5)	8: 18414769-18459953	3	1.16, 0.93, 2.6	58 ± 37 (37)

Table 3
Human-mouse comparison of the insertion sites in BCP-ALL cases

The Ensembl mouse genome annotation database (version 59) was used to find the associated mouse gene for the human genes relevant to *ETV6-RUNX1* patients (genes that did not map were hand-curated). The location of insertion sites was scored as being in the coding region of the gene ('coding') or ≤ 5K upstream of the gene ('promoter').

Mouse gene with insertion	Insertion location (relative to gene)	No. unique insertions	Dysregulation of gene in human ETV6-RUNX1 ALL lesions	Reference
Ikzf1	coding	4	In a deletion region	36*, 31**
C20orf94	coding	3	In a deletion region	7
Ebf1	coding	3	In a deletion region	7-8
Fhit	coding	3	In a deletion region	7
Chn2	coding	2	Down-regulated expression	37
Epor	promoter	2	Up-regulated expression	37-39
Flt3	promoter	2	Activating mutations	40
Mllt3	coding	2	In a deletion region	7
Nf1	coding	2	In a deletion region	7
Smarcc1	coding	2	In a deletion region	24
Tbl1xr1	coding	2	In a deletion region	7-8
Tcf4 (E2-2)	coding	2	In a deletion region	36, 41
Ankrd27	coding	1	In a deletion region	24
Arid1b	coding	1	In a deletion region	42
Atf2	coding	1	Down-regulated expression	37
Atp10a	coding	1	In a deletion region	42
B4galt1	coding	1	Down-regulated expression	37
Birc7	promoter	1	Up-regulated expression	38
Cd44	coding	1	Down-regulated expression	37-39
Clic5	coding	1	Up-regulated expression	38
Dpf3	coding	1	In a deletion region	7
Eif2s1	coding	1	Down-regulated expression	37
Fbn2	coding	1	Up-regulated expression	38
Flnb	coding	1	Down-regulated expression	37
Fyn	coding	1	In a deletion region	36*
Grik2	coding	1	In a deletion region	7
Hmg20a	coding	1	Up-regulated expression	38
Jak1	coding	1	Expression up-regulated	37
Lef1	coding	1	In a deletion region	7
Lztfl1	coding	1	In a deletion region	24
Myo10	coding	1	Up-regulated expression	38
Nr3c1	coding	1	In a deletion region	7

Mouse gene with insertion	Insertion location (relative to gene)	No. unique insertions	Dysregulation of gene in human ETV6-RUNX1 ALL lesions	Reference
Nr3c2	coding	1	In a deletion region	7
Pbef1 (Nampt)	coding	1	In a deletion region	36
Pde4b	coding	1	In a deletion region	41
Pdlim1	coding	1	Down-regulated expression	37
Ptpn2	coding	1	Down-regulated expression	37
Ptprk	coding	1	Up-regulated expression	37-38
Rap1b	coding	1	In a deletion region	42
Rb1	coding	1	In a deletion region	7-8
Rhpn2	promoter	1	In a deletion region	24
Tcf3 (E2A)	promoter	1	In a deletion region	36 *
Tcf12	coding	1	In a deletion region	42
Thada	coding	1	In a deletion region	7
Usp9x	coding	1	Down-regulated expression	37
Yipf7	coding	1	In a deletion region	41
Ywhaq	coding	1	In a deletion region	41
Zcchc7	coding	1	In a deletion region	8, 24

* reported in childhood ALL (not necessarily *ETV6-RUNX1* positive patients).

** *IKZF1* deletion outside of the BCR-ABL context.